Application of Least-Squares Variance Component Estimation to GPS Observables

A. R. Amiri-Simkooei[1]; P. J. G. Teunissen[2]; and C. C. J. M. Tiberius[3]

Abstract: This contribution can be seen as an attempt to apply a rigorous method for variance components in a straightforward manner directly to GPS observables. Least-squares variance component estimation is adopted to assess the noise characteristics of GPS observables using the geometry-free observation model. The method can be applied to GPS observables or GNSS observables in general, even when the navigation message is not available. A realistic stochastic model of GPS observables takes into account the individual variances of different observation types, the satellite elevation dependence of GPS observables precision, the correlation between different observation types, and the time correlation of the observables. The mathematical formulation of all such issues is presented. The numerical evidence, obtained from real GPS data, consequently concludes that these are important issues in order to properly construct the covariance matrix of the GPS observables. Satellite elevation dependence of variance is found to be significant, for which a comparison is made with the existing elevation-dependent models. The results also indicate that the correlation between observation types is significant. A positive correlation of 0.8 is still observed between the phase observations on L1 and L2.

DOI: 10.1061/(ASCE)0733-9453(2009)135:4(149)

CE Database subject headings: Geometry; Correlation; Least squares method; Surveys; Variance analysis.

Introduction

A realistic stochastic model of the GPS observables is a prerequisite for the many of modern applications. Noise characteristics of the GPS observables have recently been assessed by Amiri-Simkooei and Tiberius (2007), Amiri-Simkooei et al. (2006, 2007), Bischoff et al. (2005, 2006), Tiberius and Kenselaar (2000, 2003), Teunissen et al. (1998), Brunner et al. (1999), Hartinger and Brunner (1999), Wang et al. (1998, 2002), and Satirapod et al. (2002). The unknowns of the stochastic model need to be determined to properly weigh the contribution of the heterogeneous data to the final result. This leads to the minimum variance estimators using the functional model.

The previous work, carried out to assess the noise characteristic of GPS observables, is usually based on simplified formulations of the variance component methods. The importance of the present contribution relies not only on the intermediate steps to make a proper structure of the stochastic model but also on the direct application of variance component estimation (VCE) methods to GPS observables. We make use of the least-squares variance component estimation (LS-VCE), in a straightforward manner, to assess the noise characteristics of GPS observables. For this purpose, the GPS geometry-free observation model (GFOM) will be employed.

The objective of this contribution is threefold. First, we present the functional and stochastic model of the GPS GFOM. Using the Kronecker product, a more realistic stochastic model that includes the satellite elevation dependence of the GPS observables, correlation between observation types, and time correlation of the observables is presented. Second, we explain our strategy for the estimation (using LS-VCE) and presentation (for better interpretation) of the variance and covariance components. Finally, we apply LS-VCE to the geometry-free model using real data and interpret the results. Correlation between different observation types and satellite elevation dependence of the GPS observable precision will in particular be studied.

GPS Geometry-Free Observation Model

The geometry-based observation model (GBOM) is the usual mathematical model for solving high-precision positions from phase and code observations using a relative GPS receiver setup. The relative receiver-satellite geometry plays a crucial role and has a significant effect on the precision of the parameters of interest—the relative receiver position, for instance. The GFOM dispenses this receiver-satellite geometry: this linear model solves for the receiver-satellite ranges instead of positions. The GFOM is one of the simplest approaches for the estimation of integer GPS double differenced (DD) ambiguities. The terminology "geometry-free model" and "geometry-based model" is due to Teunissen and introduced in Teunissen (1997a,b,c,d). For the comparison of GBOM and GFOM, we refer to Teunissen (1997a,b,c,d) and Odijk (2008).

[1]Delft Institute of Earth Observation and Space Systems (DEOS), Faculty of Aerospace Engineering, Delft Univ. of Technology, Kluyverweg 1, 2629 HS Delft, The Netherlands; and Dept. of Surveying Engineering, The Univ. of Isfahan, 81744 Isfahan, Iran (corresponding author). E-mail: a.amirisimkooei@tudelft.nl

[2]Delft Institute of Earth Observation and Space Systems (DEOS), Faculty of Aerospace Engineering, Delft Univ. of Technology, Kluyverweg 1, 2629 HS Delft, The Netherlands; and Dept. of Spatial Sciences, Curtin Univ. of Technology, U1987, Perth, Australia.

[3]Delft Institute of Earth Observation and Space Systems (DEOS), Faculty of Aerospace Engineering, Delft Univ. of Technology, Kluyverweg 1, 2629 HS Delft, The Netherlands.

Note. This manuscript was submitted on January 10, 2008; approved on May 11, 2009; published online on October 15, 2009. Discussion period open until April 1, 2010; separate discussions must be submitted for individual papers. This paper is part of the ***Journal of Surveying Engineering***, Vol. 135, No. 4, November 1, 2009. ©ASCE, ISSN 0733-9453/2009/4-149–160/$25.00.

The favorable precision of the carrier-phase observations can be fully exploited for relative positioning if the ambiguities are estimated and kept *fixed* at their integer values. The use of the GFOM does offer some advantages. Foremost of these advantages is its ease that stems from the linearity of the observation model and its independence of satellite orbit information. The GFOM is also very versatile, as it allows the estimation of ambiguities even if observations for only two satellites are available and even if both receivers are moving. Moreover, ambiguities estimated with the GFOM are also known to be free from residual tropospheric delay in the observations, as these delays are automatically lumped with the satellite-receiver ranges. Therefore, for some applications like data analysis and ionosphere monitoring, the geometry-free approach does have its appeal.

The GFOM consists of two parts: the functional model and the stochastic model (following subsections). The functional model relates the observations to the parameters of interest, whereas the stochastic model describes the precision and the mutual correlation between the observations.

Functional Model

The geometry-free functional model is based on the nonlinearized DD dual frequency pseudorange and carrier-phase observation equations. Consider two receivers r and j simultaneously observing the same satellites s and k. For a zero and a (very) short baseline (10 m), we may neglect the dispersive DD ionospheric delay as this effect can be completely canceled out for a zero baseline and significantly reduced for a short baseline. Therefore, the DD dual frequency pseudorange observation equations are (Teunissen and Kleusberg 1998)

$$\underline{p}_{rj,L}^{sk}(t_i) = \rho_{rj,L}^{sk}(t_i) + \underline{e}_{rj,L}^{sk}(t_i) \tag{1}$$

where $(.)_{rj}^{sk}$=abbreviation for $(.)_{rj}^{k}-(.)_{rj}^{s}=(.)_{j}^{k}-(.)_{r}^{k}-((.)_{j}^{s}-(.)_{r}^{s})$; p denotes the "observed" DD pseudoranges on the L1 or L2 frequency, e.g., C1 and P2; ρ denotes the combination of all nondispersive effects; L=either L1 or L2 frequency; e denotes the pseudorange measurement errors on the L1 or L2 frequency; and t_i indicates the time instant or epoch to which the observations refer. The underscore indicates "randomness."

The most important difference between the phase and the code observations is the entry of an integer DD carrier-phase ambiguity in the phase observation equations. Expressed in units of distance (m) rather than in cycles, the DD carrier-phase observation equations read

$$\underline{\phi}_{rj,L}^{sk}(t_i) = \rho_{rj,L}^{sk}(t_i) + \lambda_L a_{rj,L}^{sk} + \underline{\epsilon}_{rj,L}^{sk}(t_i) \tag{2}$$

where ϕ denotes the observed DD carrier-phase on the L1 or L2 frequency; λ denotes the wavelength; a denotes the integer carrier-phase ambiguities on the L1 or L2 frequency; and ϵ denotes the carrier-phase measurement errors on the L1 or L2 frequency. The dual frequency DD pseudorange and carrier-phase observation equations can be summarized in the following linear system of equations:

$$E\begin{bmatrix} \underline{p}_{rj,1}^{sk}(t_i) \\ \underline{p}_{rj,2}^{sk}(t_i) \\ \underline{\phi}_{rj,1}^{sk}(t_i) \\ \underline{\phi}_{rj,2}^{sk}(t_i) \end{bmatrix} = \begin{bmatrix} 1 & 0 & 0 \\ 1 & 0 & 0 \\ 1 & \lambda_1 & 0 \\ 1 & 0 & \lambda_2 \end{bmatrix} \begin{bmatrix} \rho_{rj}^{sk}(t_i) \\ a_{rj,1}^{sk} \\ a_{rj,2}^{sk} \end{bmatrix} \tag{3}$$

where E denotes the expectation operator; the expectation of the measurement errors is assumed to be zero. This system of observation equations, which belongs to two receivers simultaneously observing two satellites, makes the single epoch geometry-free functional model. It is of course possible to include, in the functional model, the observations to more than two satellites or even the observations of more than two receivers. We restrict ourselves to the observations of two receivers and to more than two satellites.

The preceding functional model over K epochs can be summarized in a convenient vector-matrix notation as (still for two satellites)

$$E\begin{bmatrix} \underline{p}_1 \\ \underline{p}_2 \\ \underline{\phi}_1 \\ \underline{\phi}_2 \end{bmatrix} = \begin{bmatrix} I_K & 0 & 0 \\ I_K & 0 & 0 \\ I_K & u\lambda_1 & 0 \\ I_K & 0 & u\lambda_2 \end{bmatrix} \begin{bmatrix} \rho \\ a_1 \\ a_2 \end{bmatrix} \tag{4}$$

with $u=[1,1,\cdots,1]^T$ and I_K=identity matrix. If one, in one step, obtains a least-squares solution of the above, fixes the DD carrier-phase ambiguities to their integer values by using the least-squares ambiguity decorrelation adjustment (LAMBDA) method [see Teunissen (1993, 1995)] and ignores the stochastic behavior of the integer valued ambiguities, one, in the next step, will be able to simplify the above observation equations by subtracting from the observation vector a constant vector, namely, $[0\ \ 0\ \ \lambda_1\check{a}_1 u^T\ \ \lambda_2\check{a}_2 u^T]^T$, with $\check{a}_1$ and $\check{a}_2$ the least-squares integer valued ambiguities. Then, on the right hand side of the preceding equation, there will remain only the identity matrices of the design matrix.

Stochastic Model

For a single observation epoch and dual frequency undifferenced pseudorange and carrier-phase observations, a simple stochastic model is

$$D(\underline{y}) = \mathrm{diag}(\sigma_{p_1}^2, \sigma_{p_2}^2, \sigma_{\phi_1}^2, \sigma_{\phi_2}^2) \tag{5}$$

where D denotes the dispersion operator; and $\sigma_{p_i}^2$ and $\sigma_{\phi_i}^2$, $i=1,2$ denote the variances of the undifferenced pseudorange and carrier-phase observables. At this moment, the correlation between the observations is assumed to be absent. Moreover, for the sake of simplicity, in some applications, the observations on the L1 and L2 frequencies are assumed to have a constant and the same precision, i.e., $\sigma_{p_1}^2=\sigma_{p_2}^2=\sigma_p^2$ and $\sigma_{\phi_1}^2=\sigma_{\phi_2}^2=\sigma_\phi^2$. This, however, may not be the case in general (see next section).

We aim to assess the noise characteristics of GPS observables using a linear and simple GFOM. We apply LS-VCE to the stochastic part of the geometry-free model. The construction of the covariance matrix (for undifferenced observables) starts from a scaled unit matrix per observation type and takes place in different steps for the DD observables. The following suppositions regarding the noise of the GPS observables are considered:

1. The precision of the observations is assumed to be different for different observation types on different frequencies (e.g., $\sigma_{p_1} \neq \sigma_{p_2}$);
2. The observables on the L1 and L2 frequencies (both for pseudorange and carrier phase) may or may not be correlated. We estimate the correlations between observation types;
3. Satellite elevation dependence of the observables precision will be considered. We consider different variances for different satellites;

4. The formulation of time correlation of the observables is presented, however, in this contribution, we will not estimate time correlation; and
5. The correlation between different channels/satellites is assumed to be absent for all observation types [see Tiberius and Kenselaar (2003)].

Realistic Stochastic Models

The formulation of the stochastic model in the previous subsection is considered to be rudimentary and unrealistic for high-precision GPS positioning applications. In this section, we derive the formulation of the realistic stochastic model that forms the basis of our analysis. For such a stochastic model, two main issues need to be addressed: time dependent and time invariant characteristics. For the time instants t_i and t_j the (cross-time) covariance is given by (Teunissen 1997e)

$$E[\underset{\sim}{e}_p(t_i)\underset{\sim}{e}_\phi(t_j)] = \sigma_{p\phi}q(t_i,t_j) \tag{6}$$

where $q(t_i,t_j)$ captures all time-dependent characteristics such as time correlation and the satellite elevation dependence and so does $\sigma_{p\phi}$ for the invariant characteristics.

Time correlation is considered to be stationary and we assume that it is a function of the time difference rather than the absolute time instants. This, however, does not hold for the satellite elevation dependence of the GPS observables. The precision of the GPS observables changes with time. We may then use only one epoch of observations or a couple of adjacent epochs (e.g., 10 epochs), for which the precision remains unchanged. We now elaborate these issues in detail.

Satellite Elevation Dependence

Here we aim to consider the observable precision of a single channel. Instead of using a predefined elevation-dependent model, we consider individual variances for different satellites located at different elevation angles. This can be used to evaluate the correctness of the elevation-dependent models.

If, in addition to the satellites s and k, we now assume that the receivers r and j are also simultaneously tracking the satellite l, the other DD pseudorange is

$$\underset{\sim}{p}_{rj,L}^{sl}(t_i) = \rho_{rj,L}^{sl}(t_i) + \underset{\sim}{e}_{rj,L}^{sl}(t_i) \tag{7}$$

in which satellite s has been considered as reference. Assuming that the correlation between channels is absent, for each observation type, one may consider different precision for different channels. The covariance matrix of the undifferenced pseudorange observables then reads (two receivers)

$$Q = \mathrm{diag}(\sigma_{p_s}^2\sigma_{p_s}^2\sigma_{p_k}^2\sigma_{p_k}^2\sigma_{p_l}^2\sigma_{p_l}^2) \tag{8}$$

The application of the error propagation law to the DD pseudoranges Eq. (7) yields

$$Q_y^D = JQJ^T = \Sigma_E = 2\begin{bmatrix} \sigma_{p_s}^2+\sigma_{p_k}^2 & \sigma_{p_s}^2 \\ \sigma_{p_s}^2 & \sigma_{p_s}^2+\sigma_{p_l}^2 \end{bmatrix} \tag{9}$$

where the 2×6 matrix J=DD operator

$$J = \begin{bmatrix} 1 & -1 & -1 & 1 & 0 & 0 \\ 1 & -1 & 0 & 0 & -1 & 1 \end{bmatrix} \tag{10}$$

One can simplify the above covariance matrix if one assumes the same precision for different channels, i.e., $\sigma_{p_s}^2=\sigma_{p_k}^2=\sigma_{p_l}^2=\sigma_p^2$ and hence one can estimate one variance component for each observation type. In general, one needs to estimate three variance components (here for three satellites) for each observation type, i.e.

$$Q_y^D = \begin{bmatrix} 2 & 2 \\ 2 & 2 \end{bmatrix}\sigma_{p_s}^2 + \begin{bmatrix} 2 & 0 \\ 0 & 0 \end{bmatrix}\sigma_{p_k}^2 + \begin{bmatrix} 0 & 0 \\ 0 & 2 \end{bmatrix}\sigma_{p_l}^2 \tag{11}$$

where the variance components $\sigma_1=\sigma_{p_s}^2$, $\sigma_2=\sigma_{p_k}^2$, and $\sigma_3=\sigma_{p_l}^2$ of the three satellites observed at different elevation angles are to be estimated. The above structure can be employed for all observation types, for k satellites and for K epochs [see Eq. (21)].

We may use the estimated variance components to obtain the parameters of two predefined elevation-dependent models, namely

$$\text{Model I}: \sigma = a_1 + a_2 e^{-\theta/\theta_0} \tag{12}$$

given by Eueler and Goad (1991) and

$$\text{Model II}: \sigma = \frac{b_1}{\sin\theta + b_2} \tag{13}$$

given by Parkinson and Spilker (1996), where σ=standard deviation of the observables and θ and θ_0=elevation angles of the satellite and a reference elevation angle, respectively. The parameters a_1, a_2, b_1, and b_2 are to be obtained using the estimated variance components.

Time Correlation of Observables

We now explain time correlation of the GPS observables and derive the structure of its stochastic model. Consider only two epochs of observations for one observation type (as before, two receivers simultaneously tracking three satellites). The covariance matrix of undifferenced observables becomes

$$Q_y = \begin{bmatrix} \sigma_{(1)}^2 Q & \sigma_{(12)}Q \\ \sigma_{(12)}Q & \sigma_{(2)}^2 Q \end{bmatrix} = \Sigma_T \otimes Q \tag{14}$$

with the unknown matrix

$$\Sigma_T = \begin{bmatrix} \sigma_{(1)}^2 & \sigma_{(12)} \\ \sigma_{(12)} & \sigma_{(2)}^2 \end{bmatrix} \tag{15}$$

where $\sigma_{(1)}^2$ and $\sigma_{(2)}^2$=variance components of the first and second epoch, respectively; $\sigma_{(12)}$=covariance between the two epochs; $\otimes$=Kronecker product of two matrices; and Q is given by Eq. (8). From the 12 observations above, one can create four DD equations, two DD for the first epoch, and two DD for the second epoch. The application of the error propagation law gives the covariance matrix of the DD observations as

$$Q_y^D = \begin{bmatrix} J & 0 \\ 0 & J \end{bmatrix}\begin{bmatrix} \sigma_{(1)}^2 Q & \sigma_{(12)}Q \\ \sigma_{(12)}Q & \sigma_{(2)}^2 Q \end{bmatrix}\begin{bmatrix} J^T & 0 \\ 0 & J^T \end{bmatrix} \tag{16}$$

which simplifies to

$$Q_y^D = \begin{bmatrix} \sigma_{(1)}^2\Sigma_E & \sigma_{(12)}\Sigma_E \\ \sigma_{(12)}\Sigma_E & \sigma_{(2)}^2\Sigma_E \end{bmatrix} = \Sigma_T \otimes \Sigma_E \tag{17}$$

where $\Sigma_E=JQJ^T$ is given by Eq. (9).

This structure can be used for all observation types, for k satellites, and for K epochs [see Eq. (21)]. For K epochs, the matrix Σ_T contains $K(K+1)/2$ unknown (co)variance components. If the observations are equidistant in time, the stationarity of the GPS observations implies that the elements on each negative-sloping diagonal of Σ_T are equal (a symmetric Toeplitz matrix). The (co)variance component $\sigma_{(ij)}$ is then a function of the time difference $\tau=|j-i|$, namely, $\sigma_{(ij)}=\sigma_\tau=\sigma_{|j-i|}$. For example, for the entries of the main diagonal, one has $\sigma_{(1)}^2=\sigma_{(2)}^2=\ldots=\sigma_{(K)}^2=\sigma_0$. The number of unknown auto-(co)variance components will then get reduced to K [see Eq. (23)].

Cross Correlation of Observables

We now consider the correlation between different observation types. When dealing with four observation types, one needs to estimate 10 (co)variance components, namely, four variances and six covariances.

Consider the following covariance matrix for two types of undifferenced observations (e.g., single frequency), namely, pseudorange and carrier phase (as before, two receivers simultaneously tracking three satellites, one epoch)

$$Q_y=\begin{bmatrix}\sigma_p^2 Q & \sigma_{p\phi}Q\\ \sigma_{p\phi}Q & \sigma_\phi^2 Q\end{bmatrix}=\Sigma_C\otimes Q \tag{18}$$

with the unknown matrix

$$\Sigma_C=\begin{bmatrix}\sigma_p^2 & \sigma_{p\phi}\\ \sigma_{p\phi} & \sigma_\phi^2\end{bmatrix} \tag{19}$$

The application of the error propagation law to the DD form of the code and phase observations gives rise to the following covariance matrix:

$$Q_y^D=\begin{bmatrix}\sigma_p^2\Sigma_E & \sigma_{p\phi}\Sigma_E\\ \sigma_{p\phi}\Sigma_E & \sigma_\phi^2\Sigma_E\end{bmatrix}=\Sigma_C\otimes\Sigma_E \tag{20}$$

where $\Sigma_E=JQJ^T$ is given by Eq. (9).

With four observation types, one needs to estimate 10 (co)variance components, namely, four variances and six covariances. Strictly speaking, not all unknown components are estimable (specifically with the geometry-free model). The maximum number of estimable parameters is six, e.g., four variances and two covariances or just six covariances, etc. [see Amiri-Simkooei (2007), p. 63]. The other issue as to the estimability is due to the fact that two observation types are much more precise than the others, namely, carrier phase when compared with the pseudoranges. This will cause the stochastic model to be ill-posed. That is, the estimated components of the precise observations are highly correlated and poorly estimable. To handle this, one can assume the same variance for both carrier-phase observations on L1 and L2.

To summarize, when dealing with four observation types as with GPS, we note that only four components are precisely estimable, namely, one (co)variance component for carrier-phase observations and all three (co)variance components for pseudorange observations. When we deal with five observation types, e.g., L1, L2, C1, P1, and P2, seven components are precisely estimable, namely, one (co)variance component for carrier-phase observations and all three (co)variance components of the code observations. This is related to the ill-posedness of the stochastic model, which is explained by Amiri-Simkooei (2007).

Complete Structure of Stochastic Model

Based on the formulations of the previous subsections, we now present the complete structure of the stochastic model of the GPS observables for

- k number of satellites (i.e., $[1],[2],\ldots,[k]$);
- K epochs of observations, hence, $\tau=(0),(1),\ldots,(K-1)$; and
- more observation types, e.g., L1, L2, C1, and P2.

We assume that the structure of time correlation and satellite elevation dependence are identical for all observation types. With these assumptions one can show that the stochastic model of the DD GPS observables is of the form (two receivers)

$$Q_y^D=\Sigma_C\otimes\Sigma_T\otimes\Sigma_E \tag{21}$$

where

$$\Sigma_C=\begin{bmatrix}\sigma_{p_1}^2 & \sigma_{p_1p_2} & \sigma_{p_1\phi_1} & \sigma_{p_1\phi_2}\\ \sigma_{p_1p_2} & \sigma_{p_2}^2 & \sigma_{p_2\phi_1} & \sigma_{p_2\phi_2}\\ \sigma_{p_1\phi_1} & \sigma_{p_2\phi_1} & \sigma_{\phi_1}^2 & \sigma_{\phi_1\phi_2}\\ \sigma_{p_1\phi_2} & \sigma_{p_2\phi_2} & \sigma_{\phi_1\phi_2} & \sigma_{\phi_2}^2\end{bmatrix} \tag{22}$$

consists of 10 unknowns and represents cross correlation of the observables

$$\Sigma_T=\begin{bmatrix}\sigma_{(0)} & \sigma_{(1)} & \cdots & \sigma_{(K-1)}\\ \sigma_{(1)} & \sigma_{(0)} & \cdots & \sigma_{(K-2)}\\ \vdots & \vdots & \ddots & \vdots\\ \sigma_{(K-1)} & \sigma_{(K-2)} & \cdots & \sigma_{(0)}\end{bmatrix} \tag{23}$$

consists of K (co)variances and represents time correlation of the observables and

$$\Sigma_E=2\begin{bmatrix}\sigma_{[1]}^2+\sigma_{[2]}^2 & \sigma_{[1]}^2 & \cdots & \sigma_{[1]}^2\\ \sigma_{[1]}^2 & \sigma_{[1]}^2+\sigma_{[3]}^2 & \cdots & \sigma_{[1]}^2\\ \vdots & \vdots & \ddots & \vdots\\ \sigma_{[1]}^2 & \sigma_{[1]}^2 & \cdots & \sigma_{[1]}^2+\sigma_{[k]}^2\end{bmatrix} \tag{24}$$

consists of k variances and represents satellite elevation dependence of the observables precision. Compared with the diagonal structure for the matrices Σ_C, Σ_T, and Σ_E, used by many researchers, the formulation presented here is considered to be more realistic as it incorporates different noise components into the stochastic model. The unknown variance and covariance components are to be estimated using LS-VCE. Eq. (21) with Eqs. (22)–(24) form the basis of our analysis using LS-VCE.

Finally, a few comments on the nature of the stochastic model introduced in Eq. (21) are in order. The use of the Kronecker product $\otimes$ implies that the structure of time correlation and satellite elevation dependence is identical for all observation types. This can be but may not always be the case. Braasch and VanDierendonck (1999) presented models where the variances of both phase and code observations are inversely proportional to the signal to noise ratio (S/N; more precisely carrier to noise density ratio). This indicates, for a given epoch, that the Kronecker-product structure is valid but the S/N changes with time (e.g., due to elevation changes) and so do the phase and code variances. Therefore, over long time spans, Eq. (21) is valid only for satellites above a certain elevation angle and over short time spans, with all satellites, Eq. (21) is valid only for a limited number of adjacent epochs (small K). The structure of time correlation introduced by Σ_T in Eq. (23) is assumed to be identical for both code and phase observations. The code and phase variances are proportional to the code and phase tracking loop bandwidths (Braasch and VanDierendonck 1999), which can respectively induce (different) time correlation on code and phase observables. An even more realistic model may therefore introduce different time correlation structures for code and phase observations.

Estimation of Variance and Covariances

Least-Squares Variance Component Estimation

We now present the formulation of LS-VCE. Consider the linear model of observation equations

$$E(\underline{y}) = Ax; \quad D(\underline{y}) = Q_y = \sum_{k=1}^{p} \sigma_k Q_k \tag{25}$$

where $\underline{y} = m \times 1$ vector of observables; $x = n \times 1$ vector of unknown parameters; $A = m \times n$ design matrix; and $Q_y = m \times m$ covariance matrix of the observables. E and D = expectation and the dispersion operators, respectively. The unknown (co)variance components σ_k (of Q_y) are to be estimated using LS-VCE. The LS-VCE of σ then reads: $\hat{\underline{\sigma}} = N^{-1}\underline{l}$, where the entries of the $p \times p$ matrix N and the $p \times 1$ vector l are (Teunissen and Amiri-Simkooei 2008)

$$n_{kl} = \frac{1}{2} tr(Q_k Q_y^{-1} P_A^{\perp} Q_l Q_y^{-1} P_A^{\perp}) \tag{26}$$

and

$$\underline{l}_k = \frac{1}{2} \underline{y}^T Q_y^{-1} P_A^{\perp} Q_k Q_y^{-1} P_A^{\perp} \underline{y} \tag{27}$$

with $P_A^{\perp} = I - A(A^T Q_y^{-1} A)^{-1} A^T Q_y^{-1}$ an orthogonal projector. The inverse of N, i.e., $Q_{\hat{\sigma}} = N^{-1}$, gives the covariance matrix of the variance and covariance estimators. For more information, its implementation and dealing with the general form $Q_y = Q_0 + \Sigma_{k=1}^{p} \sigma_k Q_k$, we may refer to Teunissen and Amiri-Simkooei (2006) and Amiri-Simkooei (2007).

The LS-VCE is a powerful method for the estimation of the stochastic model parameters in which the σ_k's can be estimated in an iterative manner. To make the analysis faster and to reduce the memory usage of the VCE methods, we now introduce the multivariate linear model. This multivariate analysis method can accordingly be adopted to the other existing VCE methods such as best invariant quadratic unbiased estimator [see Koch (1999); Schaffrin (1983)], minimum norm quadratic unbiased estimator [see Rao (1971); Sjöberg (1983)], and restricted maximum likelihood estimator [see Koch (1986)].

Multivariate Linear Model

The procedure proposed here aims to reduce the computational load and memory usage of the variance component estimation. Theoretically, one can estimate the (co)variance components using only a few epochs of observations but they are not guaranteed to provide an appropriate precision for the estimates. In order to improve the precision of the estimators, one usually likes using all available observations. Because of the special structure of the covariance matrix of observables and the design matrix, the final estimators can be easily obtained.

Consider the $m \times m$ covariance matrix of the observables $\underline{y}$ as $Q = \Sigma_{k=1}^{p} \sigma_k Q_k$. Now this model is repeated r times $i = 1, \ldots, r$, where the unknown parameters are allowed to vary between the groups. Moreover, the measurements of different groups are assumed to be uncorrelated. This model can be applied to the GFOM when: (1) we split the observations into r groups or categories and (2) time correlation of observables (and hence between the groups) is absent. Such a multivariate model (repeated model) is of the form

$$E\begin{bmatrix} \underline{y}^{(1)} \\ \underline{y}^{(2)} \\ \vdots \\ \underline{y}^{(r)} \end{bmatrix} = \begin{bmatrix} A & 0 & \cdots & 0 \\ 0 & A & \cdots & 0 \\ \vdots & \vdots & \ddots & \vdots \\ 0 & 0 & \cdots & A \end{bmatrix} \begin{bmatrix} x^{(1)} \\ x^{(2)} \\ \vdots \\ x^{(r)} \end{bmatrix} \tag{28}$$

with the stochastic model

$$D\begin{bmatrix} \underline{y}^{(1)} \\ \underline{y}^{(2)} \\ \vdots \\ \underline{y}^{(r)} \end{bmatrix} = Q_y = \begin{bmatrix} Q & 0 & \cdots & 0 \\ 0 & Q & \cdots & 0 \\ \vdots & \vdots & \ddots & \vdots \\ 0 & 0 & \cdots & Q \end{bmatrix} \tag{29}$$

where $\underline{y}^{(i)}$ and $x^{(i)}$ = observable vector and the unknown vector of group i, respectively. The same design matrix A appears for each group but the unknowns in x are allowed to vary from group to group. Note that a single matrix Q in Eq. (29) has the form $Q = \Sigma_C \otimes \Sigma_T \otimes \Sigma_E$ of Eq. (21).

If one substitutes, in the multivariate model, the observable vector $\underline{y} \leftarrow \text{vec}([\underline{y}^{(1)} \ldots \underline{y}^{(r)}])$, the design matrix $A \leftarrow I_r \otimes A$ and the covariance matrix $Q_y \leftarrow I_r \otimes Q$ into Eqs. (26) and (27), one can prove that the final estimates are obtained by averaging the groupwise estimates

$$\hat{\sigma} = \frac{1}{r} \sum_{i=1}^{r} \hat{\sigma}^{(i)}, \quad \text{or} \quad \hat{\sigma}_k = \frac{1}{r} \sum_{i=1}^{r} \hat{\sigma}_k^{(i)}, \quad k = 1, \ldots, p \tag{30}$$

with the covariance matrix

$$Q_{\hat{\sigma}} = \frac{1}{r} N^{-1} \tag{31}$$

where N = normal matrix of a single group and $\hat{\sigma}^{(i)}$ = (co)variance components of the ith group. This shows that the unknown (co)variance components σ_k can be estimated as the arithmetic mean of the individual estimates. Such estimators have been introduced and used by Tiberius and Kenselaar (2003) and Schön and Brunner (2008) to assess the noise characteristics of the GPS observables. For more information on the multivariate linear model we refer to Amiri-Simkooei (2009).

When a model repeats every 1 s then a model consisting of 10 s (10 is arbitrary) of such data (a 10-epoch group) will occur every 10 s. We have already tested the temporal correlation of the GPS receivers involved in the analysis. The results show that the longest time correlation (worst case for receiver Trimble 4000 SSi) of the GPS observables is about 10 s. For the multivariate model introduced above, we now assume that the covariance matrix Q is the same for all 10-epoch groups, as in Eq. (29). This is our strategy for handling a full hour of GPS data.

Presentation and Interpretation of Results

It is convenient to demonstrate the numerical estimates such that they are readily understandable. We now derive simple formulas for standard deviation estimators and correlation coefficients as well as their precision only for the reason of *presentation*.

Let $\hat{\sigma}_i^2 = \hat{\sigma}_{ii}$ and $\sigma_{\hat{\sigma}_i^2} = \sigma_{\hat{\sigma}_{ii}}$ be the variance estimator and its standard deviation, respectively. We can apply the square root to the variance estimator, which gives the standard deviation estimator $\hat{\sigma}_i = \sqrt{\hat{\sigma}_i^2} = \sqrt{\hat{\sigma}_{ii}}$. The precision of the variable $\hat{\sigma}_i$, namely, $\sigma_{\hat{\sigma}_i}$, is derived by applying the error propagation law to this nonlinear function

$$\sigma_{\hat{\sigma}_i} \approx \frac{\sigma_{\hat{\sigma}_i^2}}{2\hat{\sigma}_i} = \frac{\sigma_{\hat{\sigma}_{ii}}}{2\hat{\sigma}_i} \tag{32}$$

where both $\hat{\sigma}_i$ and $\sigma_{\hat{\sigma}_{ii}}$ are given.

When the covariance estimate $\hat{\sigma}_{ij}(\mathrm{m}^2)$ and two variance estimates $\hat{\sigma}_{ii}(\mathrm{m}^2)$ and $\hat{\sigma}_{jj}(\mathrm{m}^2)$ are given, one may present the correlation coefficient instead of the covariance estimate. To obtain the variance of the correlation coefficient $\hat{\rho}_{ij} = \hat{\sigma}_{ij}/(\sqrt{\hat{\sigma}_{ii}}\sqrt{\hat{\sigma}_{jj}})$, we apply the error propagation law to the linearized form of $\hat{\rho}_{ij}$

$$\sigma^2_{\hat{\rho}_{ij}} = JQ^{ij}_{\hat{\sigma}}J^T \tag{33}$$

where the 3×3 matrix $Q^{ij}_{\hat{\sigma}}$ denotes the covariance matrix of the estimators $\hat{\sigma}_{ij}$, $\hat{\sigma}_{ii}$, and $\hat{\sigma}_{jj}$, which is given by LS-VCE. The diagonal elements of $Q^{ij}_{\hat{\sigma}}$ (i.e., $\sigma^2_{\hat{\sigma}_{ij}}$, $\sigma^2_{\hat{\sigma}_{ii}}$, $\sigma^2_{\hat{\sigma}_{jj}}$) are the variances of the estimators and the off-diagonal elements are the covariances between estimators. The Jacobi vector J is given as

$$J = \hat{\rho}_{ij}\left[\frac{1}{\hat{\sigma}_{ij}} \frac{-1}{2\hat{\sigma}_{ii}} \frac{-1}{2\hat{\sigma}_{jj}}\right] \tag{34}$$

Numerical Results and Discussions

Experiment Description

We now apply the LS-VCE method to real data and interpret the results. Three data sets were used. The first data set is the Delfland 99 campaign, carried out in an open meadow area near Delft, the Netherlands. A 1-h Ashtech Z-XII3 and Trimble 4000 SSi zero baseline data set from April 9, 1999 are considered (08:00:00–08:59:59 UTC), with 10 and eight satellites and five and four observation types, respectively, i.e., C1-P1-P2-L1-L2 and C1-P2-L1-L2 and a 1-s interval. In the sequel, for the reason of convenience, the receivers are simply called "Ashtech receiver" and "Trimble receiver." The total number of epochs is $K=3{,}600$. The second data set was obtained recently at the TU Delft GNSS observatory. A-1 h Trimble R7 (firmware v.2.32) zero baseline data set from April 10, 2008 was considered (01:00:00–01:59:59 UTC), with 10 satellites and four observation types, i.e., C1, P2 (or C2), L1, and L2 and a 1-s interval. There are three observed block IIR-M satellites in this time span, which is of particular interest in this study. For the third data set, a zero baseline was measured with two identical Septentrio AsteRx1 single frequency receivers on July 10, 2008 (23:10:00–01:10:00 UTC; 2 h). For this last experiment, data analysis of two-test Galileo satellites, GIOVE A and B, is of particular interest.

The results presented here concern zero baselines. Two receivers of the same type (four receiver-pairs Ashtech-Ashtech, Trimble-Trimble, Trimble (R7)-Trimble (R7), and Septentrio-Septentrio) were each time connected to one antenna. The antenna amplifier is responsible for a (large) part of the noise and with only one amplifier, this noise is common to both receivers, which may cause too optimistic outcomes concerning the level of measurement noise [see Amiri-Simkooei and Tiberius (2007)]. In general, when measuring an ordinary baseline with two receivers and antennas at separate locations, other effects like atmospheric and multipath effects will also play an important role. For a brief but comprehensive review, see Bona and Tiberius (2000).

The estimated (co)variances for both receivers (four receiver-pairs) over 3,600 (or 7,200) epochs, divided into 360 (720) 10-epoch groups, are presented. Our conclusion regarding implementation of LS-VCE is that only two, three, or four iterations are needed to obtain converged (co)variances. The results presented here, for all observation types, are given for the last iteration (after convergence). In all graphs, the estimates are given for each of the 360 groups. The mean estimates, presented in the tables, are based on Eq. (30).

We now estimate the variances of each observation types, the covariances (and hence correlations) between observation types, and the satellite elevation dependence of the observables precision, all based on the formulation of the stochastic model introduced in Eq. (21) for different choices of Σ_C and Σ_E. Time correlation will not be estimated in this contribution, i.e., $\Sigma_T = I$, meaning that the observations are not temporally correlated. This is indeed not an unrealistic assumption for several of the state of the art GPS receivers.

Variances of Observation Types

We have shown that the (co)variance components can be estimated using both float and fixed ambiguities in GFOM. In order to take advantage of the fixed ambiguities (less unknown parameters in the functional model) all results presented in this paper are based on "fixed ambiguities." Therefore, the results on the basis of float ambiguities are not presented.

The structure of the design matrix A is given in Eq. (4), with $K=10$. The ambiguities are estimated using the LAMBDA method (Teunissen 1995) by employing 300 epochs of observations and they are kept fixed. The success rate of the integer least-squares ambiguity estimation is good enough to ignore the randomness of the integer estimators. The vector of observations has been therefore corrected for the integer ambiguities. The design matrix in Eq. (4) simplifies to $A = [I \ I \ I \ I]^T$. Using the DD observations of all satellites (k satellites, $k-1$ DD) we then estimate one variance component for each observation type. For each 10-epoch group, we estimate one variance component for each observation type, neglecting the satellite elevation dependence of the observables precision, the time correlation, the covariance between channels, and the covariance between different observation types. The structure of Eq. (21) is used for the stochastic model, where in Eq. (22), Σ_C is assumed to be diagonal (only the variances are to be estimated). The DD observations of all satellites ($k-1$ DD) have been used. To overcome the ill-posedness of the stochastic model, we just estimate one single variance component for the L1 and L2 carrier-phase data ($\sigma_{\phi_1} = \sigma_{\phi_1}$).

Fig. 1 (top) shows the groupwise estimate of variances using the full hour of the data for the L1/L2 phase and P2 code observations of the Ashtech receiver. Table 1 gives the (mean) variance and standard deviation estimates as well as their precision. The results indicate that the noise of GPS observations is at submillimeter level (0.3 mm), centimeter level (6.7 cm), and decimeter level (2.2–2.3 dm) for phase, C1, and P1 and P2, respectively. The precision of these estimates are at micrometer level, submillimeter level, and millimeter level, respectively.

Fig. 1 (bottom) is similar to the top frame but now it corresponds to the Trimble receiver. The estimated variances grow up at the end of the graphs. It is due to satellite PRN 09 which is setting and has a low-elevation angle (nearly 10°). This cannot, however, be seen for the Ashtech receiver. It is due to the antenna

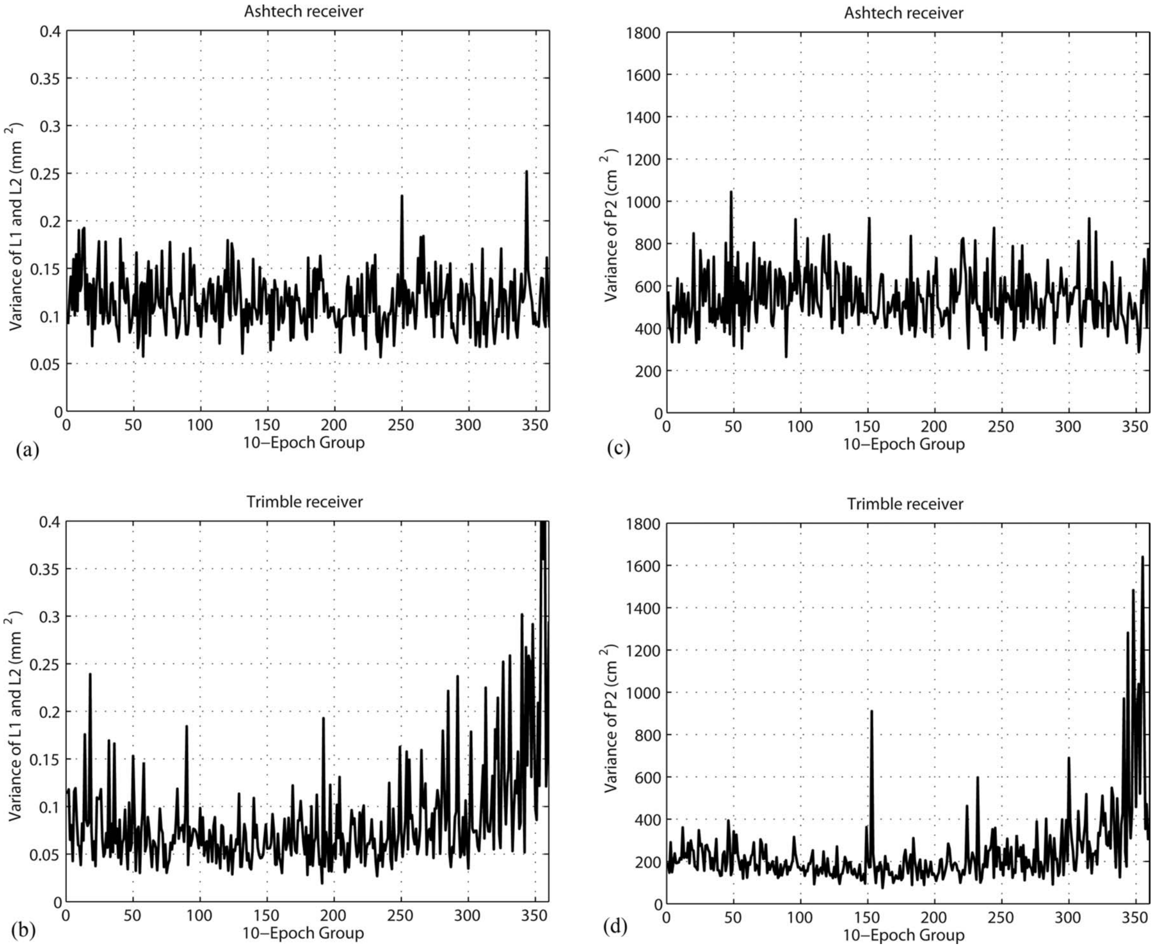

Fig. 1. Groupwise variances estimated for two types of GPS observations with fixed ambiguities (all satellites): (a and c) Ashtech receiver; (b and d) Trimble receiver; (a and b) L1 and L2 phases; and (c and d) P2 code

gain pattern (and the semicodeless tracking technique), which has a significant influence on the noise level (specially at low-elevation angles). Table 2 gives the numerical results for this receiver.

The estimated standard deviation of phase observations (combined L1 and L2) is about 0.3 mm, which looks optimistic. There are two reasons for having such a small value: (1) we deal with a zero baseline in which mainly the receiver noise is present and (2) the phase observables L1 and L2 are (positively) highly correlated but so far this was ignored (see next subsection). We now consider an example to show how an incorrect structure of the stochastic model can lead to underestimation (or overestimation) of the (co)variance components.

Consider the following linear model of observation equations with two observation types (e.g., L1 and L2 phase observations):

$$E\begin{bmatrix} \underline{y}_1 \\ \underline{y}_2 \end{bmatrix} = \begin{bmatrix} I \\ I \end{bmatrix} x, \quad D\begin{bmatrix} \underline{y}_1 \\ \underline{y}_2 \end{bmatrix} = \sigma^2 \begin{bmatrix} I & \rho I \\ \rho I & I \end{bmatrix} \tag{35}$$

where σ^2=variance of the observables and ρ=correlation coefficient between $\underline{y}_1$ and $\underline{y}_2$. If one now estimates the unknown variance σ^2 based on an uncorrelated stochastic model (i.e., $\rho=0$), one will then obtain: $\hat{\sigma}^2=(\underline{y}_1-\underline{y}_2)^T(\underline{y}_1-\underline{y}_2)/2n$, where n is the size of y_1. It is not difficult to show that $\hat{\underline{\sigma}}^2$ is not an unbiased estimator of σ^2, namely, $E(\hat{\underline{\sigma}}^2)=(1-\rho)\sigma^2 \neq \sigma^2$. It gives a too optimistic estimate for positive correlation ($\rho>0$) and a too pessimistic estimate for negative correlation ($\rho<0$). This highlights the importance of the correct structure of the stochastic model for a proper estimation of (co)variance components. Similar conclusion has been drawn by Tiberius (2001) when ignoring significant time correlation of GPS observables.

Table 1. Variance and Standard Deviation Estimates of Phase and Code Observations ($k=10$ Satellites, $k-1$ DD) as well as Their Precision for Ashtech Receiver

Observation type	$\hat{\sigma}^2$ (mm^2)	$\sigma_{\hat{\sigma}^2}$ (mm^2)	$\hat{\sigma}$ (mm)	$\sigma_{\hat{\sigma}}$ (mm)
L1/L2	0.12	0.001	0.34	0.001
C1	4,475.55	35.16	66.90	0.26
P1	49,637.10	389.94	222.79	0.88
P2	54,232.85	426.09	232.88	0.91

Table 2. Variance and Standard Deviation Estimates of Phase and Code Observations ($k=8$ Satellites, $k-1$ DD) as well as Their Precision for Trimble Receiver

Observation type	$\hat{\sigma}^2$ (mm^2)	$\sigma_{\hat{\sigma}^2}$ (mm^2)	$\hat{\sigma}$ (mm)	$\sigma_{\hat{\sigma}}$ (mm)
L1/L2	0.09	0.001	0.29	0.001
C1	8,882.24	83.09	94.25	0.44
P2	24,054.40	219.53	155.09	0.71

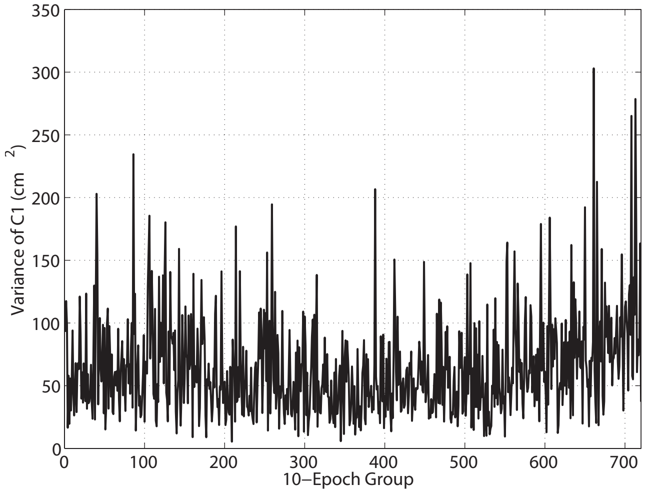

Fig. 2. Groupwise variances estimated for C1 code using two Galileo satellites (GIOVE A and B); Septentrio AsteRx1 (2 h of data divided into 720 groups)

It is worthwhile mentioning that the geometry-free model can be applied to GNSS observables, even when the navigation message is not available. This holds for the early Galileo data collected with the Septentrio AsteRx1 single-frequency receiver, which tracks Galileo satellites GIOVE A and B (third experiment, which forms one DD). The C/N0 for both GIOVE-A and B was generally in the range of 40–45 dB-Hz and GIOVE-A was setting toward the end of the observation window. Fig. 2 shows the groupwise estimate of variances using the 2 h of the C1 (C1B) code observations (720 groups), where the variance of the phase L1 has been kept fixed to 1 mm in the analysis. The average precision of C1 is about 88.3 mm.

Correlation between Observation Types

We now estimate the covariance (and hence correlation) between observation types, e.g., between C1 and P2 and between L1 and L2. Unless stated otherwise, in this subsection, the results are presented based on the DD observations to *all* satellites.

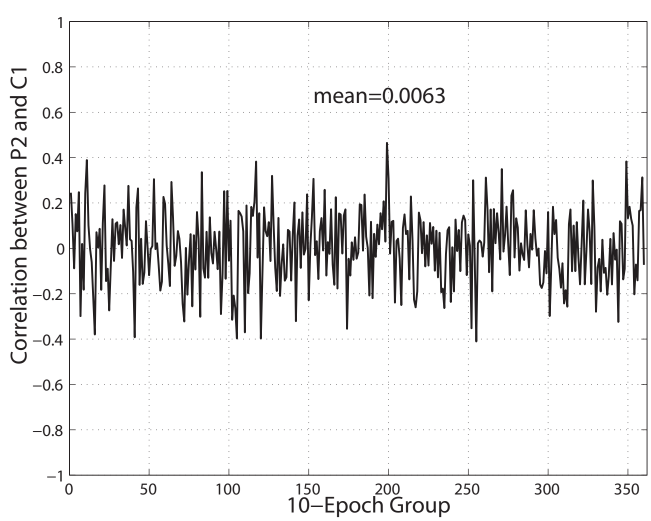

Fig. 3. Estimated correlation coefficients between C1 and P2 code observations for Ashtech receiver

Table 3. Standard Deviation Estimates as well as Their Precision for Ashtech Receiver When Considering One Variance for Phases and Six (Co)Variances for Codes in Stochastic Model (k=10 Satellites)

Observation type	$\hat{\sigma}$ (mm)	$\sigma_{\hat{\sigma}}$ (mm)
L1/L2	0.34	0.001
C1	66.90	0.26
P1	222.79	0.88
P2	232.88	0.91

Correlation between code observations. We now simultaneously estimate all the variances and covariances between code observation types (i.e., with five observation types, four variance components σ_ϕ^2, $\sigma_{p_1}^2$, $\sigma_{p_2}^2$, and $\sigma_{c_1}^2$, and three covariance components $\sigma_{c_1p_1}$, $\sigma_{c_1p_2}$, and $\sigma_{p_1p_2}$). For this purpose, the general structure introduced in Eq. (21), with Σ_C in Eq. (22), will be employed. Having obtained the covariances and variances, one may compute the correlation coefficients.

Fig. 3 shows the groupwise estimates of the (cross) correlation coefficients between C1 and P2 using the data from Ashtech receiver. The coefficients are estimated around zero and they will be averaged out. Therefore, the correlation between code observations C1 and P2 for the Ashtech receiver is not significant.

Having averaged over 360 groups, Table 3 gives the standard deviation estimates as well as their precision of the Ashtech receiver. The standard deviations estimated here coincide with the results when there are no covariances in the model (see Table 1). This implies that the estimated correlation is not significant. Table 4 gives three estimated covariances and correlation coefficients along with their precision for different code observation types. The estimated correlation coefficients are close to zero and at the level of their standard deviation and thus not significant.

Table 5 gives the standard deviation estimates of the Trimble receiver. The standard deviations estimated here do not exactly coincide with the results when there is no covariance in the model (see Table 2), which implies that the estimated correlation is significant. It thus highlights the importance of the correct structure of the stochastic model for a realistic estimation of variances. Fig. 4 shows the groupwise estimates of the (cross) correlations between C1 and P2 for the Trimble receiver. The correlations are

Table 4. Covariance and Correlation ($\hat{\sigma}_{ij}$ and $\hat{\rho}_{ij}$) Estimates of Code Observations with Their Precision for Ashtech Receiver When Considering All (Co)Variance Components in Stochastic Model (All Satellites)

Between	$\hat{\sigma}_{ij}$ (mm^2)	$\sigma_{\hat{\sigma}_{ij}}$ (mm^2)	$\hat{\rho}_{ij}$	$\sigma_{\hat{\rho}_{ij}}$
P1–P2	324.8	255.3	0.006	0.005
P1–C1	12.9	69.9	0.001	0.004
P2–C1	114.8	72.9	0.007	0.005

Table 5. Standard Deviation Estimates as well as Their Precision for Trimble Receiver When Considering One Variance for Phases and Three (Co)Variances for Codes in Stochastic Model (All Satellites)

Observation type	$\hat{\sigma}$ (mm)	$\sigma_{\hat{\sigma}}$ (mm)
L1/L2	0.29	0.001
C1	91.36	0.43
P2	172.32	0.79

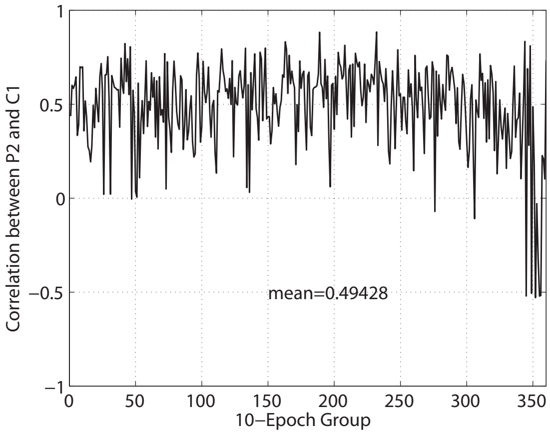

Fig. 4. Estimated correlation coefficients between C1 and P2 code observations for Trimble receiver

estimated around 0.5 and they are not averaged out. Table 6 gives the average values of the covariance and correlation coefficient. The correlation coefficient $\hat{\rho}=0.5$ between C1 and P2 is thus significant when compared to its precision.

We now make a comparison between these results with those in Tiberius and Kenselaar (2003). The standard deviation obtained for C1 and P2 are larger than those in that paper (cf. Table 5 of this contribution with those in Tab 1 of that paper). This difference makes sense because the results in Tab 1 are restricted only to the high-elevation satellites. Tiberius and Kenselaar (2003) have excluded the low-elevation satellites PRN 04, 09, and 24 for the results in Tab 1 (see, instead, Fig. 3 in that paper). A similar situation holds for the correlation between C1 and P2 (correlation of 0.76 compared to 0.5 of this contribution). The higher noise amplitudes (due to low-elevation satellites) attenuate the correlation coefficient.

A similar analysis has been repeated for the (newer) Trimble receiver (R7—second data set). The standard deviation estimates for the phase (combined L1 and L2), C1, and P2 are 0.53 mm, 13.9 cm, and 14.0 cm, respectively. The correlation coefficient between C1 and P2 is 0.1.

Table 6. Covariance and Correlation ($\hat{\sigma}_{ij}$ and $\hat{\rho}_{ij}$) Estimates between Code Observations as well as Their Precision for Trimble Receiver (All Satellites)

Between	$\hat{\sigma}_{ij}$ (mm^2)	$\sigma_{\hat{\sigma}_{ij}}$ (mm^2)	$\hat{\rho}_{ij}$	$\sigma_{\hat{\rho}_{ij}}$
P2–C1	7,066.3	114.5	0.50	0.005

Correlation between phase observations. We now consider the correlation between the phase observations L1 and L2. There are in total three (co)variances as $\sigma^2_{\phi_1}$, $\sigma^2_{\phi_2}$, and $\sigma_{\phi_1\phi_2}$. As mentioned before, only one (out of three) component is precisely estimable. So far, we assumed $\sigma_{\phi_1\phi_2}$ to be zero and $\sigma^2_{\phi}=\sigma^2_{\phi_1}=\sigma^2_{\phi_2}$. When the phase observations are highly positively correlated, one will obtain a too optimistic value for the phase precision if one ignores the correlation (e.g., the results presented in Tables 1–3).

From an independent analysis method, we found that the estimated phase precision is too optimistic (more realistic standard deviations of L1 and L2 have larger values). Using a single-epoch kinematic (geometry-based) model described by de Jong (1999), we obtained the residuals of the phase observations of different satellites. It is then possible to obtain the precision and the correlation between phase observations. Using the residuals of the satellites PRN 30, 06, and 24, with observations L1-L2-C1-P2, the phase statistics of the R7 receiver are: $\sigma_{\phi_1}=1$ mm, $\sigma_{\phi_2}=1.3$ mm, and $\rho_{\phi_1\phi_2}=0.75$. The (block IIR-M) satellites PRN 12, 31, and 29, with observations L1-L2-C1-C2, give: $\sigma_{\phi_1}=0.9$ mm; $\sigma_{\phi_2}=1.1$ mm; and $\rho_{\phi_1\phi_2}=0.80$. Similar analysis was done for the Ashtech receiver. The results are: $\sigma_{\phi_1}=0.22$ mm; $\sigma_{\phi_2}=0.48$ mm; and $\rho_{\phi_1\phi_2}=0.37$.

We now introduce the (known) precision σ_{ϕ_1} and σ_{ϕ_2} of the phase observations into the covariance matrix as the constant term Q_0, namely, $Q_y=Q_0+\sum_{k=1}^{p}\sigma_k Q_k$ and estimate the only covariance $\sigma_{\phi_1\phi_2}$. A significant positive correlation (0.72 and 0.83) is observed between L1 and L2 phase observations for the R7 receiver (Fig. 5). Also, a correlation of 0.40 was found for the Ashtech receiver.

A high correlation between phase observations has already been identified by different researches [see Bona and Tiberius (2000); Tiberius and Kenselaar (2003); Amiri-Simkooei and Tiberius (2007)]. Note that, here, the L2 phase is significantly correlated with L1 regardless the type of carrier tracking associated, i.e., either to P2 code or to C2 (L2C) code. This is in fact unexpected because the L2 phase, obtained from the L2C, could in theory be uncorrelated with L1. In principle, one can implement a tracking loop for L2C independent of L1 [see Fontana et al. (2001)].

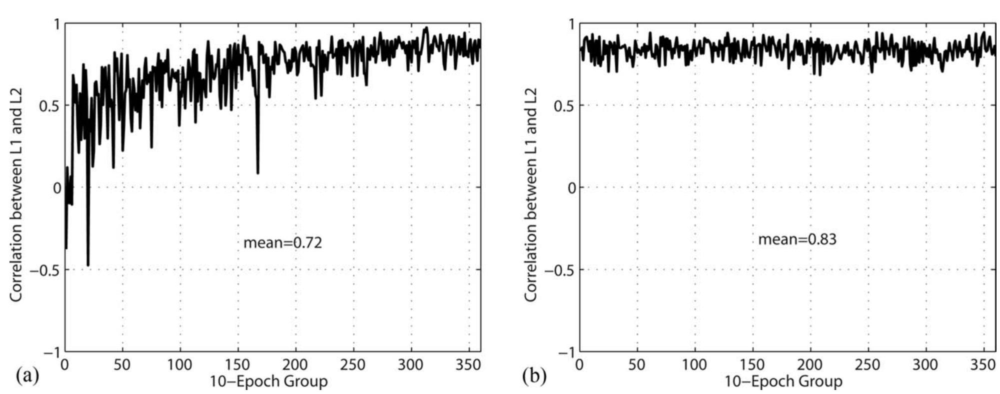

Fig. 5. Groupwise correlation coefficients between phase observations L1 and L2: (a) using data from satellites PRN 30, 06, 24 (L1-L2-C1-P2); (b) using data from (block IIR-M) satellites PRN 12, 31, 29 (L1-L2-C1-C2) , R7 receiver

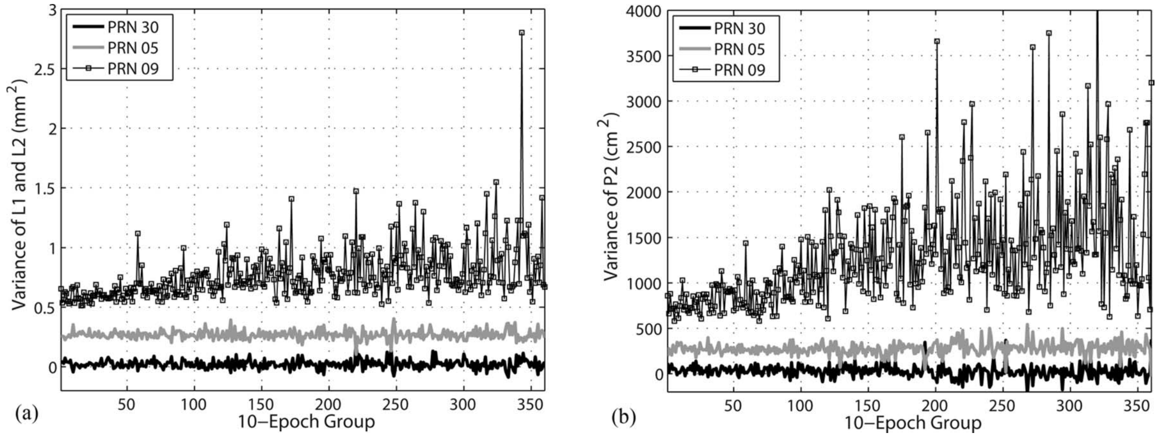

Fig. 6. Groupwise variances of satellites PRN 30, 05, and 09 estimated for L1/L2 phase [(a) shifted upward by 0.025 and 0.05 for PRN 05 and PRN 09, respectively] and P2 code; [(b) shifted upward by 0.25 and 0.5 for PRN 05 and PRN 09, respectively] observables (Ashtech receiver)

Single Channel Variances

For the evaluation of the satellite elevation dependence of the GPS observable precision, we can use the structure introduced in Eq. (21), with $k=3$ for four or five observation types ($\Sigma_T=I$). For each satellite, diagonal elements of Σ_C are estimated with the decomposition of Σ_E, given in Eq. (11). The observations from three satellites have been employed, namely, satellites PRN 30, 05 (high elevation), and 09 (low elevation) for the Ashtech receiver and satellites PRN 30, 24 (high elevation), and 06 (low elevation) with observations L1-L2-C1-P2 and PRN 31, 29 (high elevation), and 12 (low elevation) with observations L1-L2-C1-C2 for the R7 receiver. The significant correlations between the phase observations (results from previous subsection) are introduced into the stochastic model.

Fig. 6 shows the groupwise estimates of variances using the data (L1/L2 phase and P2 code) of the satellites PRN 30, 05, and 09 for Ashtech receiver. The variances estimated for satellite PRN 09, which is descending and has the lowest elevation angle, are larger than those estimated for satellites PRN 30 and 05. Also, when the elevation angle decreases, a positive trend is observed (for the last groups, on average, the estimated variances are larger than those for the first groups). The variances estimated for satellites PRN 30 and 05 are (highly) negatively correlated (Fig. 6, when one component is estimated up, the other component is estimated down). This can also be seen from the covariance matrix of the estimates (i.e., $Q_{\hat{\sigma}}=N^{-1}$, which is provided by LS-VCE), as the correlation coefficients of variances between satellites PRN 30 and 05 are $\hat{\rho}_{\phi}=-0.85$, $\hat{\rho}_{p1}=-0.93$, $\hat{\rho}_{p2}=-0.93$, and $\hat{\rho}_{c1}=-0.79$.

Table 7 gives the numerical results. The results indicate that the noise of satellites PRN 30 and 05 observations is about 0.2-mm, 3- cm, and 5-cm level for phase, C1, and P1 and P2, respectively. The precision of these estimates are at micrometer level and millimeter level for the phase and the code observations, respectively. The noise of satellite PRN 09 observations, with the lowest elevation angle, is about 0.5-mm, 8-cm, and 27–28-cm level for phase, C1, and P1 and P2, respectively.

We now estimate only one variance for each observation type of the high-elevation satellites (PRN 30 and 05). Again, the structure introduced in Eq. (11) was employed but now, the first and second variances are considered to be identical ($\sigma_1=\sigma_2$). This overcomes the problem of the negative variances (due to the lack of high redundancy) obtained for some components (Fig. 6 PRN 30 and 05) and also removes the high correlation between the estimates. Using this assumption, the variances were estimated (results not presented here). For satellite PRN 09 the same results as before were obtained. The combined variances estimated for satellites PRN 30 and 05 were modestly smoothed. They were approximately the simple arithmetic mean of the two previous components σ_1 and σ_2.

We now use the estimated groupwise variances of the low-elevation satellites to obtain the parameters of two predefined elevation-dependent models I and II, presented in Eqs. (12) and (13), respectively. For the R7 receiver, the data from the satellites PRN 30, 06, and 24 (L1-L2-C1-P2) and then PRN 12, 31, and 29 (L1-L2-C1-C2) were used. Fig. 7 shows the estimated variances for the two low-elevation satellites (top, PRN 06 and bottom, PRN 12) along with their best fits using models I and II. Based on the values of the overall model test (Teunissen 2000) both models seem to fit the data well. To make a statement on the superiority of these two models, one needs a longer observation time span with observations at lower elevations.

As a final remark we note that, currently, the use of L2C (C2) is not considerably preferable over the use of P2, as the variances obtained are nearly the same (Fig. 7, frames at right). This conclusion was made based on the P2 and C2 codes from two differ-

Table 7. Standard Deviation Estimates along with Their Precision for Different Observation Types of Satellites PRN 30, 05, and 09 (Ashtech Receiver)

Observation type	Satellite No.	$\hat{\sigma}$ (mm)	$\sigma_{\hat{\sigma}}$ (mm)
L1/L2	PRN 30	0.15	0.007
L1/L2	PRN 05	0.14	0.007
L1/L2	PRN 09	0.53	0.007
C1	PRN 30	25.39	1.12
C1	PRN 05	32.32	0.93
C1	PRN 09	77.76	0.98
P1	PRN 30	49.86	3.23
P1	PRN 05	48.88	3.29
P1	PRN 09	270.17	3.24
P2	PRN 30	54.07	3.36
P2	PRN 05	51.81	3.50
P2	PRN 09	283.27	3.40

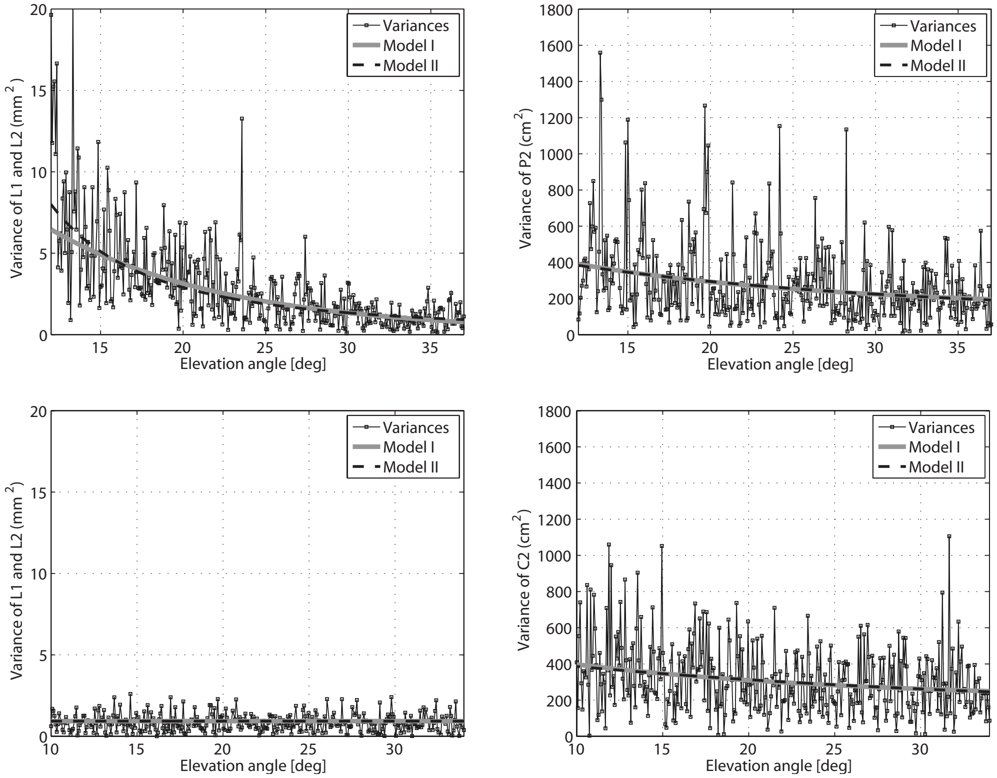

Fig. 7. Variances of phase observations (left) and code observations (right) of low-elevation satellites PRN 06 (top, P2) and PRN 12 (bottom, C2) along with their best fits of models I and II

ent satellites (for block IIR-M satellites, only C2 is available) but still located at similar elevation. The conclusion coincides also with the findings of Leandro et al. (2008). We also note that the variance of the phase observations, for the block IIR-M satellite PRN 12, is not much dependent on the elevation of the satellite (see frames at left in Fig. 7). This holds also for the correlation of L1 and L2, which remains constant in Fig. 5 (right).

Conclusions and Recommendations

The LS-VCE method was applied to the GPS GFOM using real data. The model is linear and can be easily implemented in computer code. We started by formulating the functional and stochastic model of the GPS observables. The general form of the stochastic model $Q_y^D = \Sigma_C \otimes \Sigma_T \otimes \Sigma_E$ was considered. This model includes the variance components of and the correlations between different observation types, time correlation of the observables, and the satellite elevation dependence of GPS observables precision. To obtain the minimum variance estimators of the parameters of interest and for a proper precision description of the estimators, such important issues should be taken into account in the covariance matrix of the GPS observables. This is a motivation to further study the GPS observable noise characteristics.

We showed that the precision of the GPS observables depends, to a large extent, upon the elevation of satellites (however, this was not the case for the precision of phase observations of the block IIR-M satellite PRN 12). A comparison was made with the existing satellite elevation-dependent models. Also, significant correlation between observation types was found. Among them, the correlation between code observations C1 and P2 and between phase observations L1 and L2 is remarkably significant. This can significantly affect the high-precision GPS positioning applications when it is ignored.

The huge number of observations in case of GPS is always an advantage when estimating the stochastic model parameters; the larger the redundancy of the functional model, the better the precision of the estimators in the stochastic model. When dealing with large amounts of GPS data, the computation burden of VCE methods will be drastically increased. We will have to think of efficient techniques to take advantage of large redundancy. For this purpose, the multivariate observation equation model was used in which the observations are divided into small groups. The final estimate was shown to be simply the arithmetic mean of the individual groupwise estimates.

We used the geometry-free model to assess the stochastics of GPS observables. To overcome some of the restrictions of this model (on VCE methods), apparently, the GPS geometry-based model is more fruitful. For example, it allows one to estimate the noise components of the carrier-phase observations, L1 separately from L2. This is because the redundancy of the geometry-based model is larger than that of the geometry-free model but we should also note that the geometry-free model has the advantage that it is applicable to GNSS observables even when the navigation message is not available (see Fig. 2 on the early Galileo data set).

Acknowledgments

The writers would like to acknowledge Professor T. Soler, the editor-in-chief, and three anonymous reviewers for their useful comments, which significantly improved the quality and presentation of this paper. The Australian Research Council Federation

Fellowship support of the second writer (project number FF0883188) is greatly appreciated.

References

Amiri-Simkooei, A. R. (2007). “Least-squares variance component estimation: Theory and GPS applications.” Ph.D. thesis, Delft Univ. of Technology, Delft, The Netherlands.

Amiri-Simkooei, A. R. (2009). “Noise in multivariate GPS position time-series.” *J. Geodesy, Berlin*, 83, 175–187.

Amiri-Simkooei, A. R., and Tiberius, C. C. J. M. (2007). “Assessing receiver noise using GPS short baseline time series.” *GPS Solutions*, 11(1), 21–35.

Amiri-Simkooei, A. R., Tiberius, C. C. J. M., and Teunissen, P. J. G. (2006). “Noise characteristics in high precision GPS positioning.” P. Xu, J. Liu, A. Dermanis, eds., *Proc., 6th Hotine-Marussi Symp. of Theoretical and Computational Geodesy*, Springer, Berlin, 280–286.

Amiri-Simkooei, A. R., Tiberius, C. C. J. M., and Teunissen, P. J. G. (2007). “Assessment of noise in GPS coordinate time series: Methodology and results.” *J. Geophys. Res.*, 112, B07413.

Bischoff, W., Heck, B., Howind, J., and Teusch, A. (2005). “A procedure for testing the assumption of homoscedasticity in least squares residuals: A case study of GPS carrier-phase observations.” *J. Geodesy, Berlin*, 78, 397–404.

Bischoff, W., Heck, B., Howind, J., and Teusch, A. (2006). “A procedure for estimating the variance function of linear models and for checking the appropriateness of estimated variances: A case study of GPS carrier-phase observations.” *J. Geodesy, Berlin*, 79, 694–704.

Bona, P., and Tiberius, C. C. J. M. (2000). “An experimental comparison of noise characteristics of seven high-end dual frequency GPS receiver-sets.” *Proc., IEEE PLANS2000*, Institute of Navigation (ION), Manassas, Va., 237–244.

Braasch, M. S., and VanDierendonck, A. J. (1999). “GPS receiver architectures and measurements.” *Proc. IEEE*, 87(1), 48–64.

Brunner, F. K., Hartinger, H., and Troyer, L. (1999). “GPS signal diffraction modelling: The stochastic model SIGMA-Δ model.” *J. Geodesy, Berlin*, 73, 259–267.

Eueler, H. J., and Goad, C. (1991). “On optimal filtering of GPS dual frequency observations without using orbit information.” *Bull. Geod.*, 65, 130–143.

Fontana R. D., Cheung W., Stansell T. (2001) “The modernized L2 civil signal: Leaping forward in the 21st century.” *Proc., GPS World*, 28–34.

Hartinger, H., and Brunner, F. K. (1999). “Variances of GPS phase observations: The SIGMA-ϵ model.” *GPS Solut.*, 2(4), 35–43.

de Jong, C. (1999). “A modular approach to precise GPS positioning.” *GPS Solut.*, 2(4), 52–56.

Koch, K. R. (1986). “Maximum likelihood estimate of variance components.” *Bull. Geod.*, 60, 329–338.

Koch, K. R. (1999). *Parameter estimation and hypothesis testing in linear models*, Springer, Berlin.

Leandro, R. F., Thirumurthi, T., Sükeova, L., Langley, R. B., and Santos, M. C. (2008). “Analysis of GPS L2C signal quality and its impact on PPP performance.” *Proc., ION NTM 2008*, Institute of Navigation (ION), San Diego, 1020–1031.

Odijk D. (2008). “GNSS Solutions: What does geometry-based and geometry-free mean in the context of GNSS?” *Inside GNSS*, March/April, 22–24.

Parkinson, B. W., and Spilker, J. J. (1996). *Global positioning system: Theory and applications, progress in astronautics and aerodynamics*, Vol. 163–164, American Institute of Astronautics, Washington, D.C.

Rao, C. R. (1971). “Estimation of variance and covariance components—MINQUE theory.” *J. Multivariate Anal.*, 1, 257–275.

Satirapod, C., Wang, J., and Rizos, C. (2002). “A simplified MINQUE procedure for the estimation of variance-covariance components of GPS observables.” *Surv. Rev.*, 36(286), 582–590.

Schaffrin, B. (1983). *Varianz-kovarianz-komponenten-schätzung bei der ausgleichung heterogener wiederholungsmessungen C282*, Deutsche Geodätische Kommission, Munchen, Germany (in German).

Schön, S., and Brunner, F. K. (2008). “A proposal for modelling physical correlations of GPS phase observations.” *J. Geodesy, Berlin*, 82(10), 601–612.

Sjöberg, L. E. (1983). “Unbiased estimation of variance-covariance components in condition adjustment with unknowns—A MINQUE approach.” *Zeitschrift für Vermessungswesen*, 108(9), 382–387.

Teunissen, P. J. G. (1993). “Least squares estimation of the integer GPS ambiguities.” *Proc., IAG General Meeting*, Series No. 6, Delft Geodetic Computing Centre.

Teunissen, P. J. G. (1995). “The least-squares ambiguity decorrelation adjustment: A method for fast GPS integer ambiguity estimation.” *J. Geodesy, Berlin*, 70(1–2), 65–83.

Teunissen, P. J. G. (1997a). “A canonical theory for short GPS baselines (Part I).” *J. Geodesy, Berlin*, 71(6), 320–336.

Teunissen, P. J. G. (1997b). “A canonical theory for short GPS baselines (Part II).” *J. Geodesy, Berlin*, 71(7), 389–401.

Teunissen, P. J. G. (1997c). “A canonical theory for short GPS baselines (Part III).” *J. Geodesy, Berlin*, 71(8), 486–501.

Teunissen, P. J. G. (1997d). “A canonical theory for short GPS baselines (Part IV).” *J. Geodesy, Berlin*, 71(9), 513–525.

Teunissen, P. J. G. (1997e). “GPS ambiguity resolution: Impact of time correlation, cross correlation and satellite elevation dependency.” *Stud. Geophys. Geod.*, 41, 181–195.

Teunissen, P. J. G. (2000). “Testing theory: An introduction.” Delft Univ. Press, The Netherlands, ⟨http://www.vssd.nl⟩ (Sept. 2, 2009).

Teunissen, P. J. G., and Amiri-Simkooei, A. R. (2006). “Variance component estimation by the method of least-squares.” *Proc., 6th Hotine-Marussi Symp. of Theoretical and Computational Geodesy, IAG Symposia*, Vol. 132, P. Xu, J. Liu, and A. Dermanis, eds., Springer, Berlin, 273–279.

Teunissen, P. J. G., and Amiri-Simkooei, A. R. (2008). “Least-squares variance component estimation.” *J. Geodesy, Berlin*, 82(2), 65–82.

Teunissen, P. J. G., and Kleusberg, A. (1998). “Section 7: Quality control and GPS.” *GPS for geodesy*, P. J. G. Teunissen and A. Kleusberg, eds., Springer, Berlin.

Teunissen, P. J. G., Jonkman, N. F., and Tiberius, C. C. J. M. (1998). “Weighting GPS dual frequency observations: Bearing the cross of cross-correlation.” *GPS Solut.*, 2(2), 28–37.

Tiberius C. (2001). “A univariate analysis of the impact of time correlation.” *Boll. Geod. Sci. Affini.*, 60(2001), 33–48.

Tiberius, C. C. J. M., and Kenselaar, F. (2000). “Estimation of the stochastic model for GPS code and phase observables.” *Surv. Rev.*, 35(277), 441–454.

Tiberius, C. C. J. M., and Kenselaar, F. (2003). “Variance component estimation and precise GPS positioning: Case study.” *J. Surv. Eng.*, 129(1), 11–18.

Wang, J., Stewart, M. P., and Tsakiri, M. (1998). “Stochastic modeling for static GPS baseline data processing.” *J. Surv. Eng.*, 124(4), 171–181.

Wang, J., Satirapod, C., and Rizos, C. (2002). “Stochastic assessment of GPS carrier phase measurements for precise static relative positioning.” *J. Geodesy, Berlin*, 76, 95–104.